



Radiation impact of ashes from the combustion of bottom sediments in a municipal sewage treatment plant, Czajka, located in Warsaw, Poland

Sławomir Neffe ,
Joanna Lemańska ,
Bartłomiej Fliszkiewicz ,
Sławomir Jednorog 

Abstract. The aim of the present research was to assess the radiological importance of the fly ashes generated from the incineration of sludge from the “Czajka” sewage treatment plant located in Warsaw, Poland. The γ -spectrometry technique was employed for their radiometry. The high purity germanium (HPGe) detector was mathematically energy-efficiency calibrated. The ash samples were measured two times, i.e., after 24 days and after 3 months of storage. Storage was supposed to provide a radioactive equilibrium. Radionuclides from three natural decay series, i.e., uranium–radium, uranium–actinium, and thorium, were detected in the ash samples. Apart from these, ^{40}K , ^{137}Cs , and ^7Be were also detected. The indicated levels of radionuclides do not produce radioactive hazards, regardless of the method used for further management.

Keywords: Fly ashes • Radioactivity • Sewage • Sludge combustion

Introduction

The “Czajka” Sewage Treatment Plant (Fig. 1) processes many liquid pollutants generated in the Warsaw agglomeration. The incineration plant, located in the “Czajka” plant, is one of the largest facilities of this type in Poland. Approximately 500 tons of sewage sludge is produced daily in the “Czajka” plant. The combustion process carried out in the incineration plant reduces their amount by 10 times. However, the annual amount of waste is so large that there is an urgent need to solve the problem of its disposal.

The sewage sludge incineration system of the incineration plant consists of two independent technological lines that operate in a continuous mode. Each of them is equipped with a separate furnace with a recuperator, a heat recovery boiler, and a three-stage purification system. The installation has a capacity of 24.5 t/h of wet sludge, and the incineration furnaces present use the Pyrofluid® fluidized bed technology that can burn 150 tons of dry sludge in 24 h. To manage and use the ashes produced during combustion, e.g., in agriculture as fertilizers or in construction as an additive in cement production, they should be tested, among others, for the content of radionuclides, and their levels should be assessed.

Thus, a series of fly ashes collected from the “Czajka” plant was subjected to intensive radiometric tests to accurately estimate the levels of radioactivity.

S. Neffe, B. Fliszkiewicz
Military University of Technology
Warsaw, Poland

J. Lemańska , S. Jednorog
Central Laboratory for Radiological Protection
Konwaliowa 7 St., 03-194 Warsaw, Poland
E-mail: j.lemanska@clor.waw.pl

Received: 3 October 2023
Accepted: 30 April 2024

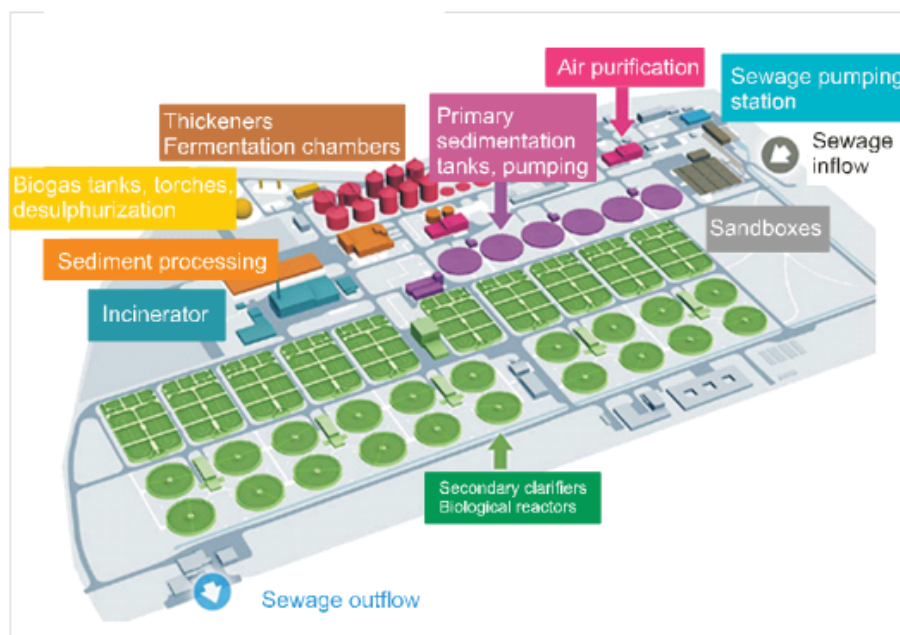


Fig. 1. Schematic of the “Czajka” sewage treatment plant located in Warsaw, Poland.

Materials and methods

Ashes sampling and composition

Totally, 17 monthly samples of fly ash, weighing ≈ 1 kg, were collected at the end of the thermal disposal line in the period from August 2022 to April 2023. They were homogenized by quartering, dried at 80°C for 6 h, and stored in closed polypropylene containers. Then laboratory samples weighing ≈ 900 g and having a density $0.77 \pm 0.04 \text{ g}\cdot\text{cm}^{-3}$ were prepared for future testing.

Energy dispersive X-ray spectroscopy (EDX) provided the average chemical composition of the tested fly ashes (Table 1). Chemical composition plays an important role during energy-efficiency calculations due to self-attenuation in the sample bulk.

Table 1. Average content in mass percentage determined by the EDX technique

Element	Average content in mass percentage
C, carbon	1.86
O, oxygen	33.99
Na, sodium	0.40
Mg, magnesium	1.60
Al, aluminum	13.15
Si, silicon	13.36
P, phosphorus	9.18
S, sulfur	0.92
K, potassium	1.33
Ca, calcium	13.93
Ti, titanium	0.70
Mn, manganese	0.25
Fe, iron	8.13
Cu, copper	0.43
Zn, zinc	0.75

The uncertainty of determining the content of the individual elements using the EDX method is smaller than 1%.

Radioactive equilibrium

Radioactive equilibrium refers to the state in which the activity of a radioactive parent nuclide and that of its radioactive daughter nuclide become equal. Radioactive equilibrium is named secular equilibrium and occurs in a radioactive decay chain only if the half-life ($T_{1/2}$) of the daughter radionuclide ($T_{1/2 \text{ progeny}}$) is much shorter than the $T_{1/2 \text{ parent}}$ of the parent radionuclide.

Let us assume that two radioactive elements compose a chain, and the first one is a parent and the second one, also radioactive, is a progeny radionuclide. Their activity varies over time in accordance with the law of decay. The activity of the progeny radionuclide $A_{\text{progeny}}(t)$ determined at time t is represented by the equation:

$$(1) \quad A_{\text{progeny}}(t) = A_{\text{parent}} \left(1 - e^{-\lambda_{\text{progeny}} t} \right)$$

where: A_{parent} is the activity of the parent radionuclide; λ_{progeny} is the decay constant.

Determination of the natural decay series radionuclides' activity

Determination of ^{238}U ($T_{1/2} = 4.468 \times 10^9$ year) activity using direct γ -ray spectrometry poses a challenge due to its long $T_{1/2}$ and low γ -ray intensity. To obtain quantitative results, it is essential to use a method based on the identification of ^{238}U decay products, such as ^{234}Th and $^{234\text{m}}\text{Pa}$ [1]. ^{228}Ra ($T_{1/2} = 5.75$ year) and its progeny radionuclide belong to the thorium decay series. It can be indicated by the activity ^{228}Ac ($T_{1/2} = 6.15$ h). Its parent radionuclide is ^{228}Ra . The last one is a progeny for ^{228}Th ($T_{1/2} = 1.9125$ year), which is the starting radionuclide for the mentioned series. ^{232}Th ($T_{1/2} = 1.40 \times 10^{10}$ year), serves as the progenitor radionuclide in the thorium

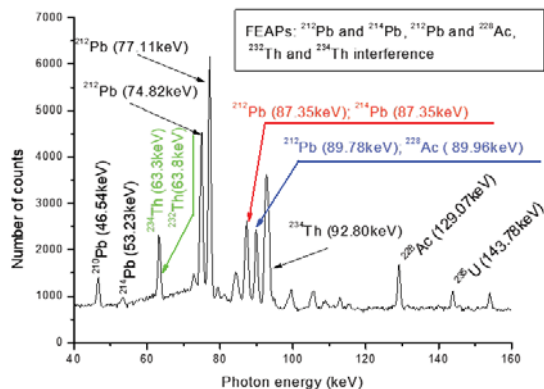


Fig. 2. Interference of radionuclides FEAPs: ²³²Th and ²³⁴Th, ²¹²Pb and ²¹⁴Pb, ²¹²Pb and ²²⁸Ac based on current results.

decay chain. Its γ -peak at 63.81 keV is interfered with by the ²³⁴Th peak at 63.29 keV, thus avoiding direct determination of ²³²Th (Fig. 2). Identification of ²³²Th is feasible via its progeny such as ²²⁸Ac, ²¹²Pb, and ²⁰⁸Tl, but this is possible only when they are in radioactive equilibrium [2]. Due to ²²⁸Ra's distinct chemical characteristics, this equilibrium does not consistently occur in environmental samples.

²³⁵U ($T_{1/2} = 7.04 \times 10^8$ year) is the starting radionuclide for the uranium-actinium decay series. The full energy absorption peaks (FEAPs) at energies of 143.77, 163.36, 185.71, and 205.31 keV could determine its radioactivity. Unfortunately, the most-intense FEAP at 185.71 keV usually interferes with the peak at 186.21 keV, resulting in the disintegration of ²²⁶Ra (Fig. 3). Thus, it is advised to determine ²³⁵U based on other noninterfering FEAPs, which are less intensive. After determining the ²³⁵U activity, we indirectly determine the part of the considered net peak area that belongs to ²²⁶Ra and next calculate its activity. However, this is not the only possible way to determine the mentioned radionuclides' activity [3].

The determination of ²¹⁰Pb radioactivity is done directly via the γ -peak at the comparatively low energy of 46.54 keV. The determination of ²²⁸Th radioactivity from the radionuclides ²¹²Pb and ²⁰⁸Tl is utilized. For the analysis, the γ -peak of ²¹²Pb at 238.63 keV is predominantly recommended. ²⁰⁸Tl radioactivity is usually easy to obtain. Radionuclides like ⁷B, ¹³⁷Cs, and ⁴⁰K do not belong to the

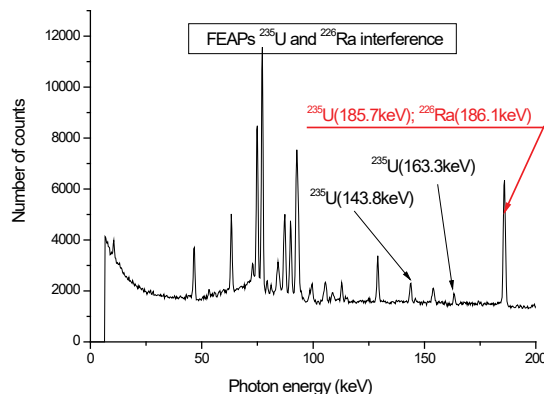


Fig. 3. Interference of ²³⁵U and ²²⁶Ra FEAPs based on current results.

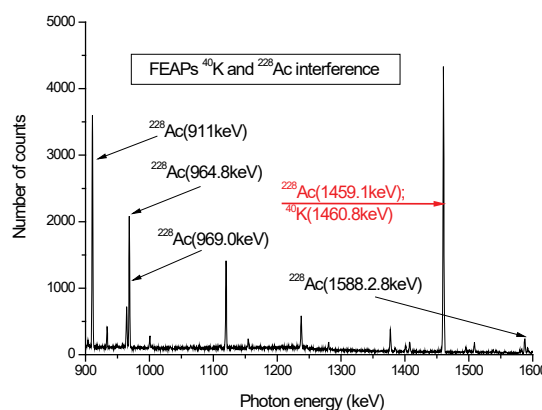


Fig. 4. Interference of ⁴⁰K and ²²⁸Ac FEAPs based on current results.

natural decay series. The initial two radionuclides can be identified using the software that typically comes with a modern γ -spectrometer. During the determination of ⁴⁰K radioactivity, it is considered that its main spectrometric line of 1460.82 keV interferes with the line of 1459.14 keV related to ²²⁸Ac disintegration (Fig. 4). Based on ²²⁸Ac activity, one can calculate the contribution to the peak area at 1460.82 keV coming from this radionuclide. The rest of the peak area is related to ⁴⁰K activity [4].

Gamma ray spectrometry

Photons were detected using an high purity germanium (HPGe) detector (coaxial, p-type, relative efficiency 33.8%, full width at half maximum (FWHM) ($E_\gamma = 1332.5$ keV) = 1.73 keV, serial number b20227, type GC3018, Canberra made), which was stored in a 100 mm Pb + 1 mm Cu shielding house and has a numerical characteristic provided by the manufacturer that allowed for mathematical energy-efficiency calibration. The multichannel analyzer Inspector and Genie2000 software were used to acquire γ -spectra and calculate the net peak area. We measured the samples and the background radiation for 24 h. Based on the nuclear data [5] and the energy-efficiency calibration result, radionuclide activity was computed in a spreadsheet, accounting for any potential FEAP interference.

Mathematical energy-efficiency calibration

The Laboratory Sourceless Calibration Software (LabSOCS®) was utilized for the numerical modeling of the photon transit within the sample and detector volume and for the mathematical energy-efficiency calibration. Geometry Composer® was utilized to describe the measurement geometry. Next, a logarithmic polynomial up to the fifth degree interpolated the pair consisting of photon energy and the corresponding registration efficiency (see Eq. (2)).

$$(2) \quad \ln \text{Eff}(E_\gamma) = \sum_{i=0}^n A_i \cdot x^i; \quad x = \ln \frac{B}{E_\gamma}$$

where: E_γ – photon's energy; $\text{Eff}(E_\gamma)$ – registration

efficiency of photons with energy E_γ ; and A_i , and B are the interpolation coefficients. In our case, the fourth-degree polynomial fit was best suited to the results.

Validation of the radiometric process

For the validation of the radiometry in terms of its effectiveness, the analytical tool integrated absolute full energy peak efficiency (IAFEPE) integral of the efficiency function $Eff(E_\gamma)$ over the detection energy range (E_{\min} – E_{\max}) was adopted [6] Eq. (3).

$$(3) \quad \text{IAFEPE} = \int_{E_{\min}}^{E_{\max}} Eff(E_\gamma) dE_\gamma$$

Sample and measurement geometries

Simplified Marinelli beaker. The first series of measurements was completed using a simplified Marinelli beaker. The ashes were placed in the container up to 1 cm from the lid. The mean mass of the ashes was ≈ 480 g. The cut view of the measurement geometry is shown in Fig. 5. It also served as the input for the MCNP calculations, leading to mathematical energy-efficiency calibration.

Simplified beaker. After completing the first series of measurements, the ash was withdrawn to a simplified beaker made of PVC, having a cone shape, and connected to the remaining part of the ash (Fig. 5). The mass of ashes increased to ≈ 660 g. Then, the beaker was suspended for 3 months, and the second series of measurements was completed. The reason for such a procedure to take place was due to the expectation of achieving a state of radioactive equilibrium for progeny radionuclides with a $T_{1/2} > 20$ days.

Results and discussion

In Figs. 2–4, a part of the γ -spectra of a representative sample of ashes is presented.

The survey included a measurement error (0.05–3.4%), an error in determining the ashes composition (1%), and a mathematical energy-efficiency calibration error (0.1%) [7]. The measurement time and weighing error can be neglected. Hence, the resultant uncertainty is 3.5%.

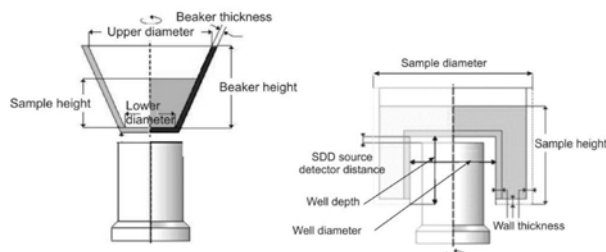


Fig. 5. The measurement geometries adopted for both series of measurements. Simplified beaker (on the left) and Marinelli beaker. Own drawing based on the Geometry Composer screen.

The calculated IAFEPE values are as follows: $\text{IAFEPE}_{\text{Marinelli beaker}} = 18.015$ keV and $\text{IAFEPE}_{\text{Simplified beaker}} = 18.325$ keV. It means that both sample geometries are comparably effective. The deterioration in the recording efficiency of the photons emitted from the simplified beaker compared to the Marinelli beaker is compensated by the increase in the mass of the sample.

Table 2 displays the specific activity of the radionuclides found in the samples. They are part of three natural decay sequences. In addition to those, we identified ^7Be , ^{40}K , and ^{137}Cs . ^{40}K is a naturally occurring radionuclide, ^7Be is cosmogenic, and ^{137}Cs is an artificial fission product. ^{137}Cs was found in the recent global fallout due to nuclear tests and accidents at nuclear reactors like Windscale, Chernobyl, and Fukushima. The activities of ^{137}Cs and ^{40}K in environmental samples monitored by Central Laboratory for Radiological Protection (CLRP) are approximately at the same levels [8]. ^7Be is produced in the solar system relatively recently and through spallation in the Earth's atmosphere. It happens on Earth due to precipitation in the form of both rain and dry fallout. Due to the unknown time that passed between the formation and its appearance in the food chain, the found radioactivity of ^7Be cannot be compared with its level in the atmosphere, surface waters, etc.

In the measured samples, we observed slightly higher levels of ^{226}Ra and ^{228}Ac in comparison with soil samples [8]. However, it is not advisable to compare the radioactivity of the ashes with that of any of the environmental samples. It is because the material from which the ashes are obtained undergo multiple metabolic, chemical, and physical transformations in food chains.

The specific activities of the samples are very similar after their long-term storage. However, this is

Table 2. The mean value of the specific activity and its standard deviation (SD) for radionuclides detected in samples of ashes from the “Czajka” plant

Radionuclide	Mean specific activity \pm SD (Bq/kg)
^{137}Cs	5 ± 2
^7Be	479 ± 98
^{40}K	417 ± 442
Uranium–radium series	
$^{234\text{m}}\text{Pa}$	$149\,881 \pm 97\,150$
^{210}Bi	$2\,762 \pm 2\,310$
^{234}Th	446 ± 395
^{214}Bi	$4\,670 \pm 2\,762$
^{210}Pb	286 ± 228
^{226}Ra	41 ± 30
Thorium series	
^{228}Ac	382 ± 239
^{212}Bi	960 ± 566
^{212}Pb	92 ± 44
^{208}Tl	15 ± 5
Uranium–actinium series	
^{235}U	5 ± 3

not the case with ^7Be , which simply disintegrates due to its relatively short $T_{1/2}$. The distribution of specific activity for radionuclides is very wide, ranging from a few becquerels for ^{235}U to tenths of a megabecquerel for $^{234\text{m}}\text{Pa}$. The reason for the relatively high $^{234\text{m}}\text{Pa}$ concentrations is unknown. However, its short $T_{1/2}$ makes the potential radiation hazard negligible.

A large variability in the content of each radionuclide was also observed. The monthly distribution of radioactivity was chaotic and does not reflect a seasonal dependence. Thus, we operate with mean values and the SD.

Conclusions

The ashes from the “Czajka” plant cannot be considered as environmental samples. The elements including those belonging to natural decay chains enter various food chains many times. Thus, their concentrations are unknown and difficult for interpretation. The concentrations of most radionuclides are different than those usually observed in environmental samples [8]. Their specific activity changes from a few parts of Bq/kg to tenths of MBq/kg. The expected dispersion of activity between the samples was up to several dozen percentage. No seasonal changes were observed across the entire series of measurements.

Fly ashes from the “Czajka” incinerator can be added to building materials or used as artificial fertilizers without causing a significant increase in radiation exposure.

Thus, one can assume the option that radiation hazards due to the utilization of ashes because of burning bottom sediments from sewage treatment plants can be neglected.

Neither the Marinelli beaker nor the simplified beaker ensured the tightness of the sample. In this way, part of the radon radionuclides could have been released from the containers. Thus, the radiative equilibrium was not entirely preserved.

ORCID

B. Filiszkiewicz  <http://orcid.org/0000-0002-1339-5879>
S. Jednorog  <http://orcid.org/0000-0003-4996-6917>

J. Lemańska  <http://orcid.org/0009-0002-4699-1586>
S. Neffe  <http://orcid.org/0000-0002-2790-6449>

References

1. Adsley, I., Backhouse, J. S., Nichols, A. L., & Toole, J. (1998). U-238 decay chain: Resolution of observed anomalies in the measured secular equilibrium between Th-234 and daughter Pa-234m. *Appl. Radiat. Isot.*, 49(9/11), 1337–1344. [https://doi.org/10.1016/S0969-8043\(97\)10070-7](https://doi.org/10.1016/S0969-8043(97)10070-7).
2. Singhal, R. K., Basu, H., Saha, S., Kumar, A., & Pimple, M. V. (2016). Estimation of ^{232}Th concentration in environmental matrices by tracking activity of major daughter products (^{212}Bi , ^{212}Pb and ^{228}Ac) with time in a hermetically sealed container. *J. Environ. Anal. Chem.*, 3(4), 1000186. DOI: 10.4172/2380-2391.1000186.
3. De Corte, F., Umans, H., Vandenberghe, D., De Wispelaere, A., & Van Den Haute, P. (2005). Direct gamma-spectrometric measurement of the ^{226}Ra 186.2 keV line for detecting $^{238}\text{U}/^{226}\text{Ra}$ disequilibrium in determining the environmental dose rate for the luminescence dating of sediments. *Appl. Radiat. Isot.*, 63(5/6), 589–598. <https://doi.org/10.1016/j.apradiso.2005.05.008>.
4. Federal Ministry for the Environment, Nature Conservation and Consumer Protection. (2018). *Procedures manual for monitoring of radioactive substances in the environment and of external radiation*. Federal Office for Radiation Protection (BfS) & Physikalisch-Technische Bundesanstalt (PTB).
5. Decay Radiation Database. (2023, February). NuDat3. [computer software]. National Nuclear Data Center. Retrieved February 21, 2023, from <https://www.nndc.bnl.gov/nudat3/help/dehelp.jsp>.
6. Jednorog, S., Klis, B., & Szewczak, K. (2024). Integrated absolute full energy peak efficiency: A measure of photon registration efficiency. *Appl. Radiat. Isot.*, 206, 111237. <https://doi.org/10.1016/j.apradiso.2024.111237>.
7. Jednorog, S., Szydłowski, A., Scholz, M., Paduch, M., & Bienkowska, B. (2012). Preliminary determination of angular distribution of neutrons emitted from PF-1000 facility by indium activation. *Nukleonika*, 57(4), 563–568.
8. Central Laboratory for Radiological Protection. (2021). *Annual Report 2020*. Warsaw: CLRP.